SUPPLEMENTARY INFORMATION

Zhixin Luo, ‡[a] Jiayi Tang, ‡[a] Zehua Wang, ‡[a] Guangming Yang,[b] Tianjiu Zhu,[ac] Zezhou Lin,[ad] San Ping Jiang[ae] and Zongping Shao[*a]

a. WA School of Mines: Minerals, Energy & Chemical Engineering (WASM-MECE), Curtin University, Perth, WA 6102, Australia.
b. State Key Laboratory of Materials-Oriented Chemical Engineering, College of Chemical Engineering, Nanjing Tech University, Nanjing 211816, China.
c. School of Chemical Engineering, The University of Queensland, QLD 4072, Australia.
d. Department of Applied Physics and Research Institute for Smart Energy, The Hong Kong Polytechnic University, Hong Kong 999077, China.
e. Foshan Xianhu Laboratory of the Advanced Energy Science and Technology Guangdong Laboratory, Foshan 528216, China.

*Corresponding author. E-mail: zongping.shao@curtin.edu.au

‡ These authors contributed equally to this work.

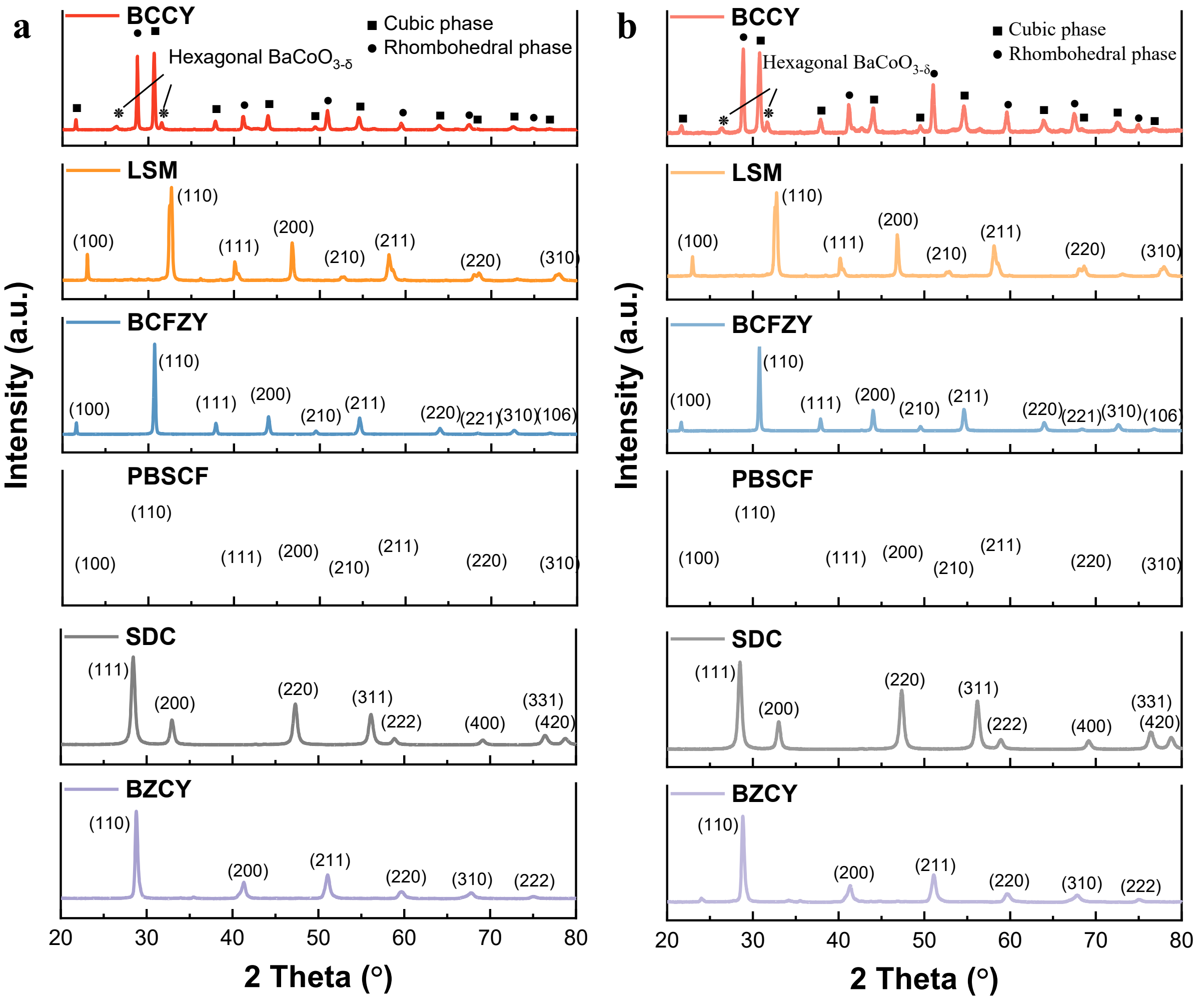

Fig. S1. XRD patterns of (a) the selected electrodes and electrolytes powders, and (b) the powders collected after the 2 h treatment under 600 °C in humified Air (40 vol.%).

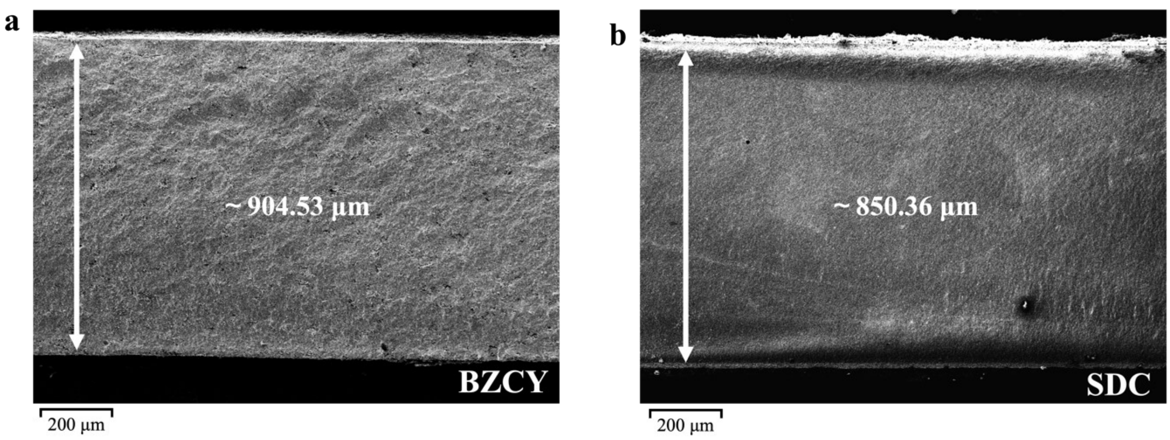

Fig. S2. SEM images of the cross-section area of the typical (a) BZCY electrolyte membrane and (b) SDC electrolyte membrane for symmetrical cells. The electrolyte membranes are densified with the average thickness of 0.90 mm for the same bath of BZCY pellets, and 0.85 mm for the same batch of SDC pellets.

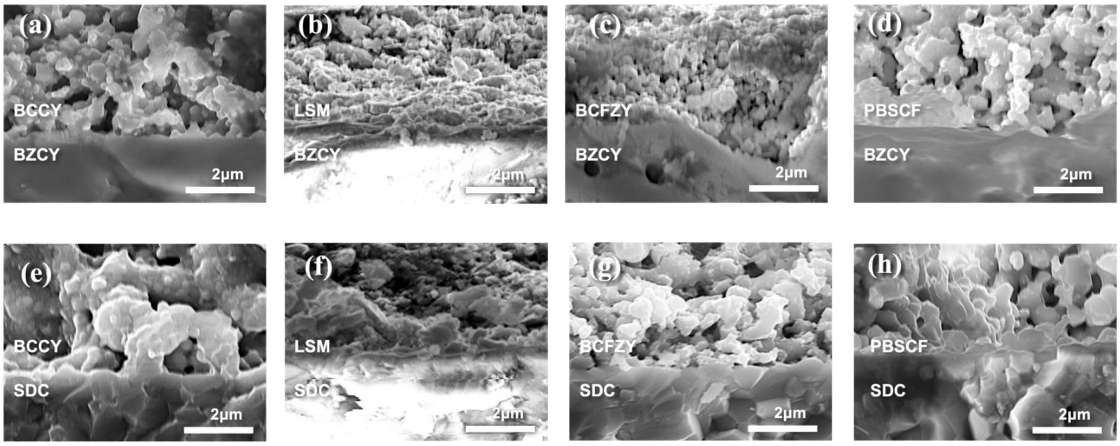

Fig. S3. SEM images of the representatives (a) BCCY-BZCY, (b) LSM-BZCY, (c) BCFZY-BZCY, (d) PBSCF-BZCY, (e) BCCY-SDC, (f) LSM-SDC, (g) BCFZY-SDC, and (h) PBSCF-SDC electrolyte-electrode interfaces of pristine symmetric cells.

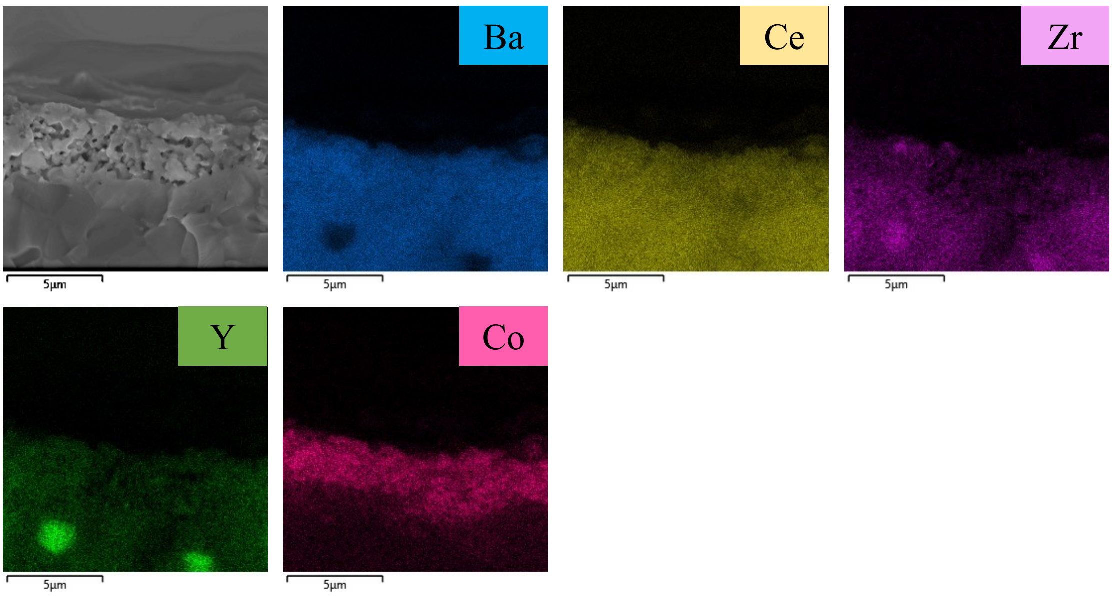

Fig. S4. The EDS mapping images of the interface of BCCY electrode on BZCY electrolyte after EIS test.

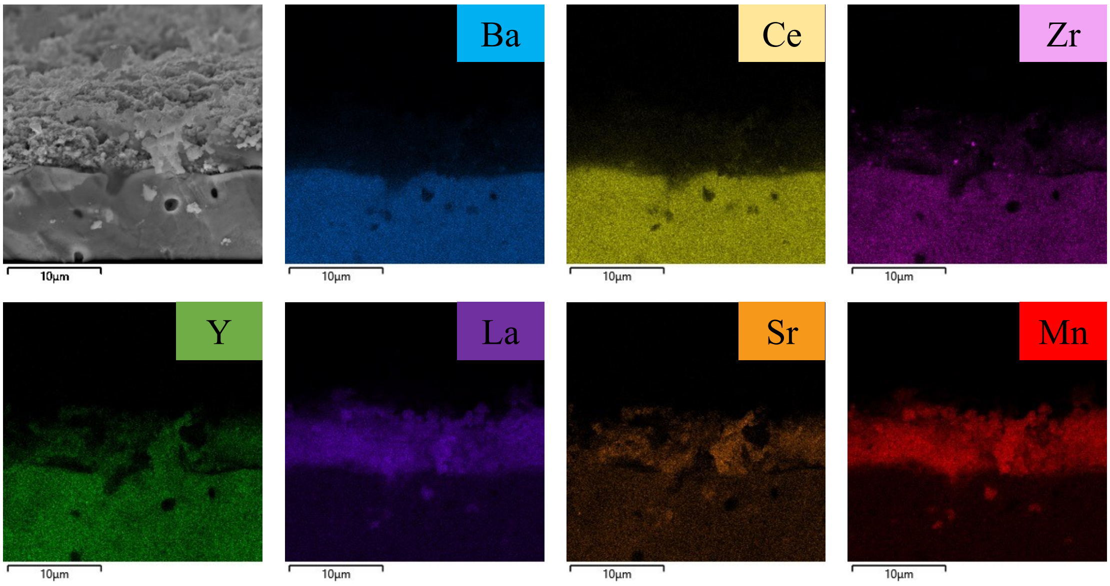

Fig. S5. The EDS mapping images of the interface of LSM electrode on BZCY electrolyte after EIS test.

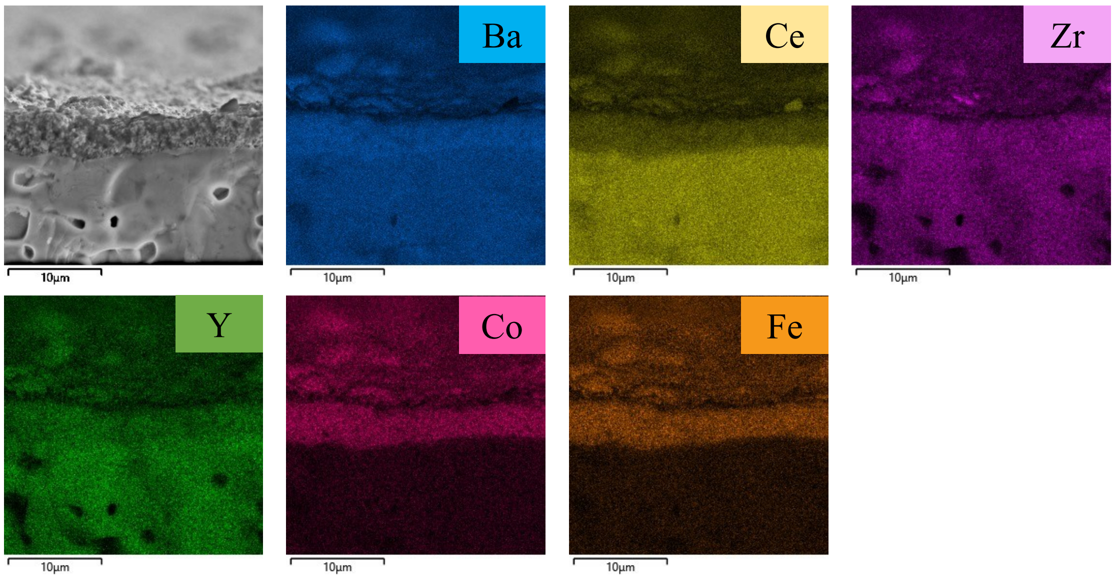

Fig. S6. The EDS mapping images of the interface of BCFZY electrode on BZCY electrolyte after EIS test.

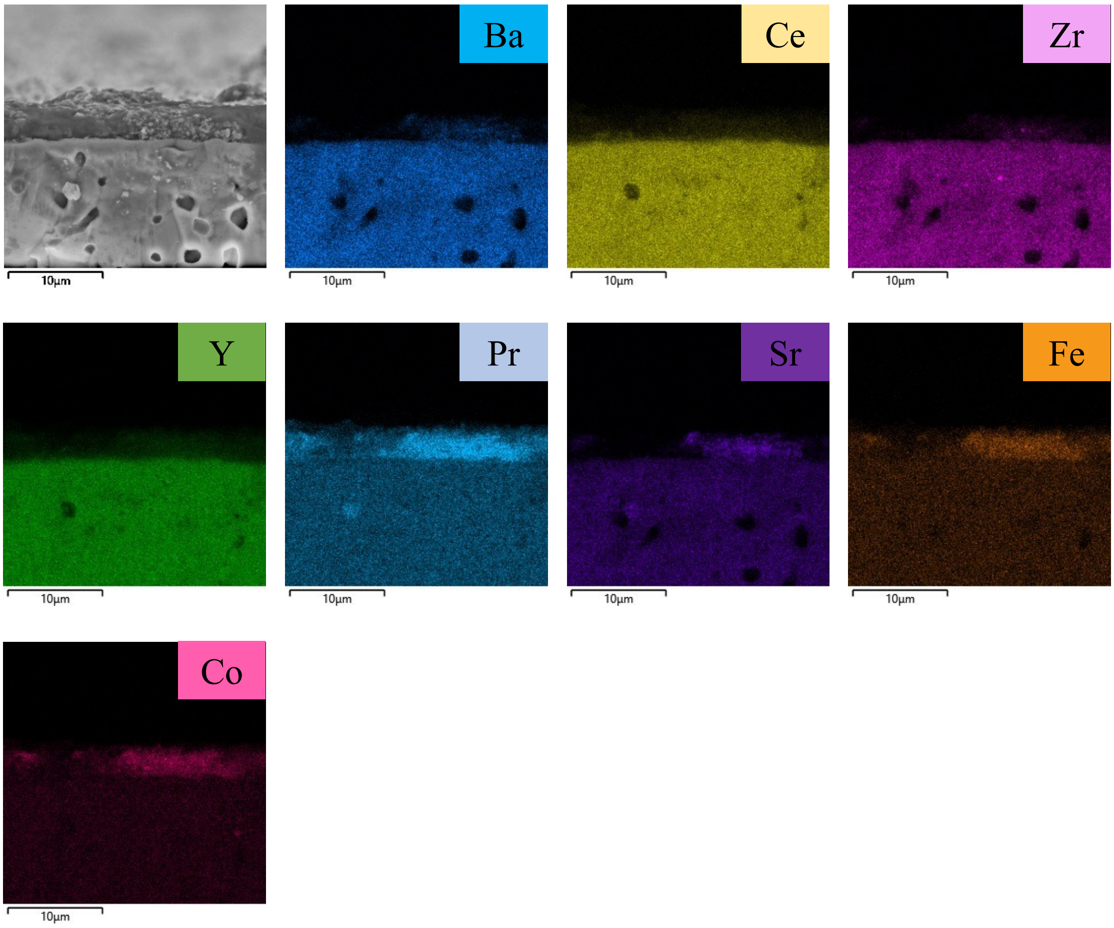

Fig. S7. The EDS mapping images of the interface of PBSCF electrode on BZCY electrolyte after EIS test.

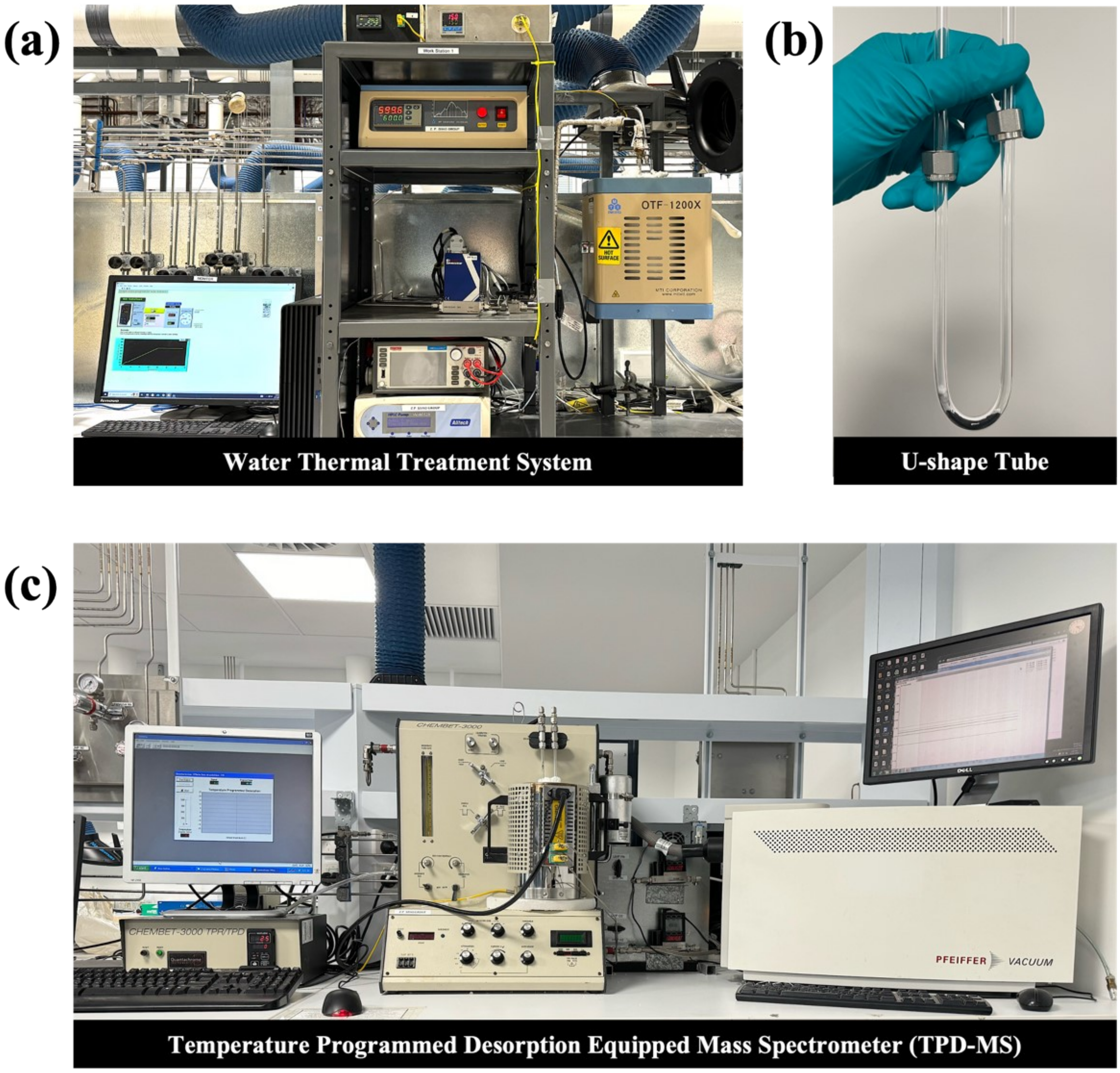

Fig. S8. Devices involved for H_2O-TPD during the experiment to study water content in the materials.

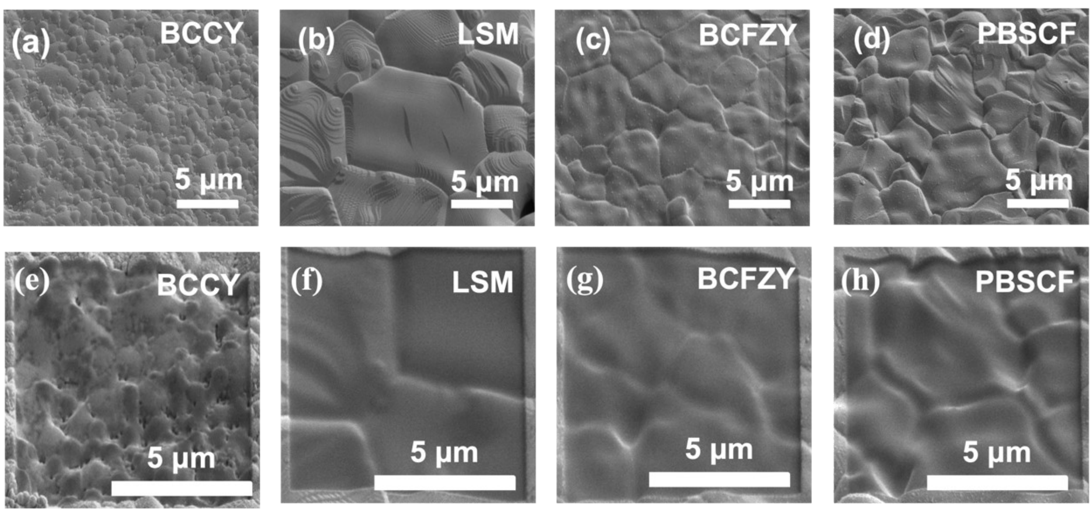

Fig. S9. Surficial SEM images of sintered (a) BCCY, (b) LSM, (c) BCFZY and (d) PBSCF before running the TOF-SIMS sputtering. Surficial SEM images of sintered (e) BCCY, (f) LSM, (g) BCFZY and (h) PBSCF after sputtering.

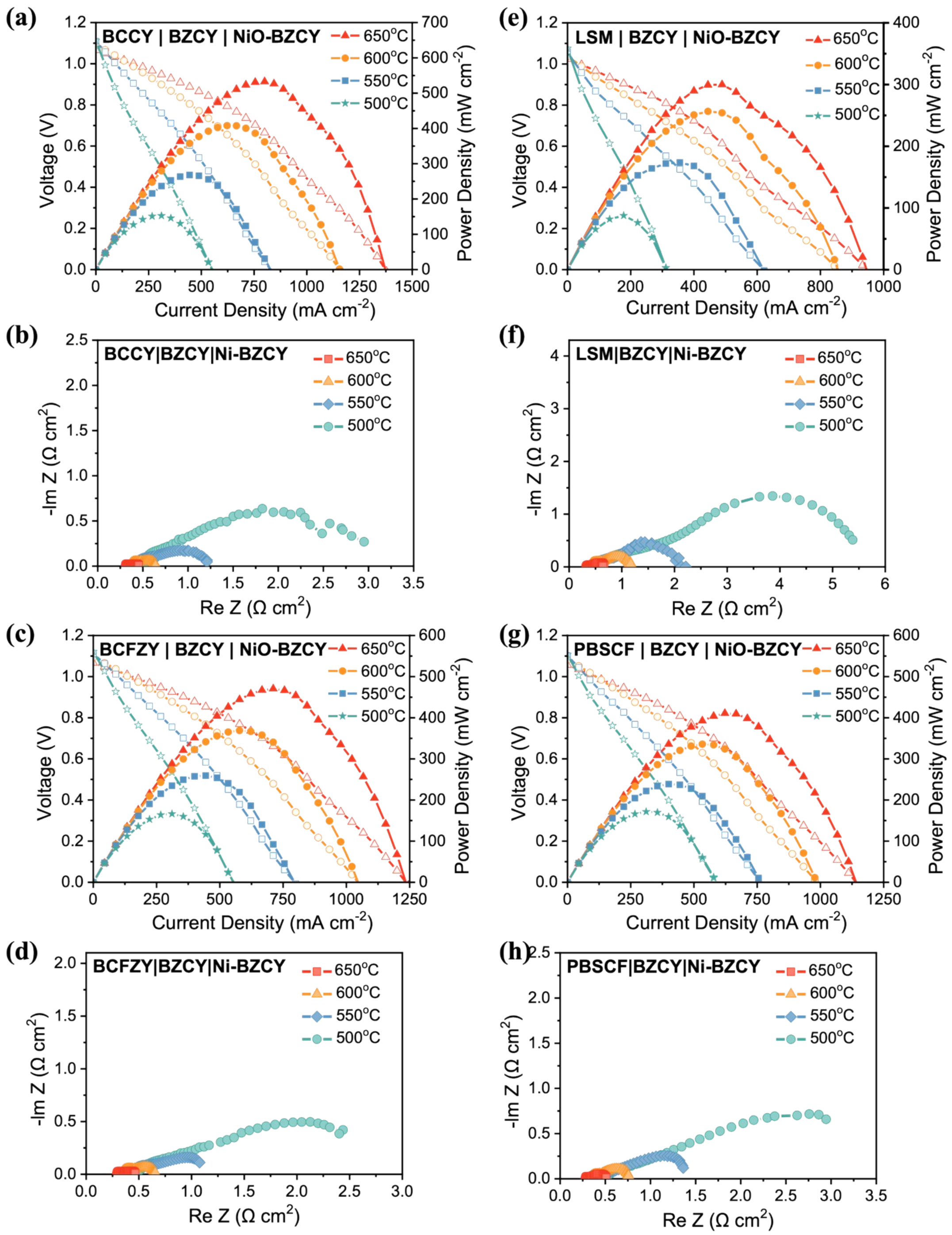

Fig. S10. BCCY|BZCY| Ni-BZCY (a) single cell I-V curve (b) single cell EIS measurement. LSM|BZCY| Ni-BZCY (c) single cell I-V curve (d) single cell EIS measurement. BCFZY|BZCY| Ni-BZCY (e) single cell I-V curve (f) single cell EIS measurement. PBSCF|BZCY| Ni-BZCY single cell (g) single cell I-V curve (h) single cell EIS measurement.

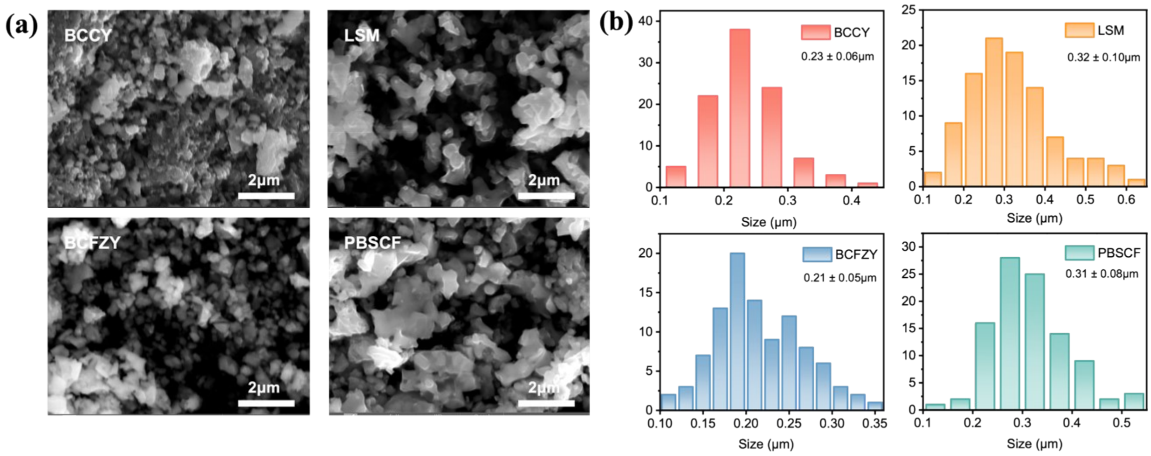

Fig. S11. Electrode particle sizes. (a) The SEM mapping images of the four calcinated electrode powder, (b) The calculated average particle sizes and size distribution of four electrode powders.

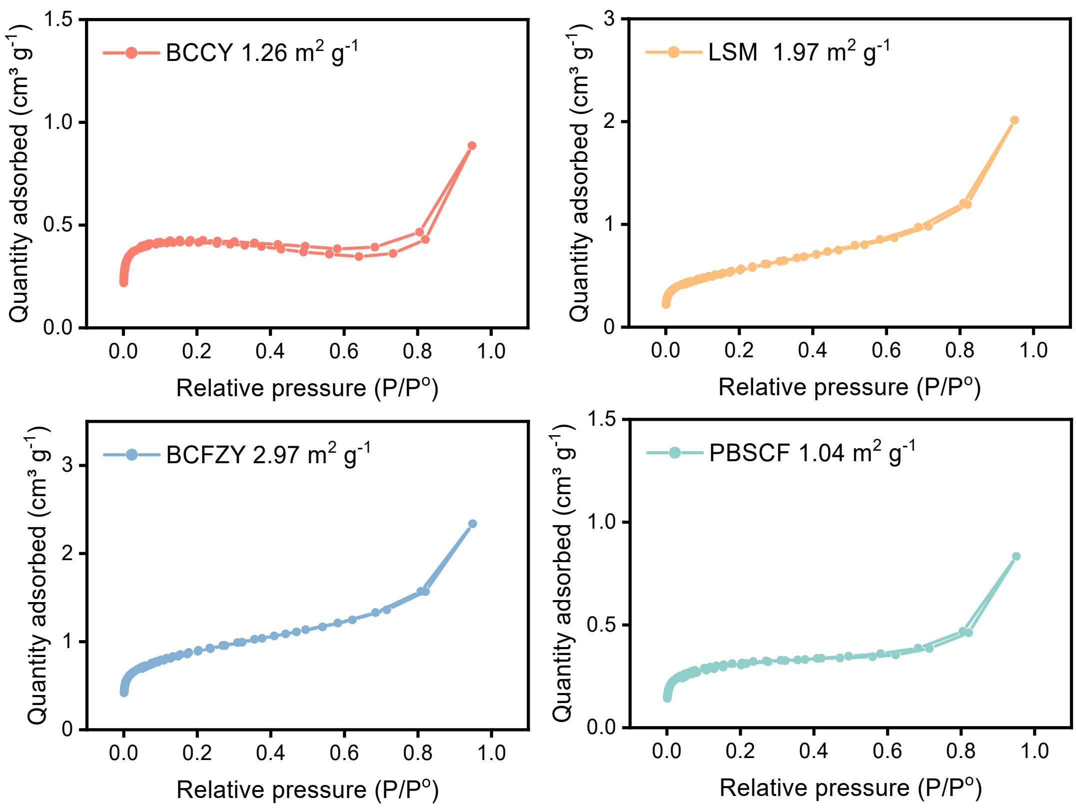

Fig. S12. The nitrogen adsorption-desorption isotherms at STP of four electrode powders and corresponding BET surface areas.

Table S1. Comparison of the different electrode ASRs measured based on BZCY/BZCYYb electrolyte symmetric cells in the temperature range of 550 to 650 °C in this work with the estimated values reported in the literature.

Cathode	Electrolyte	Atmosphere & humidity	Temperature (°C)	ASR (Ω cm^2)	Ref.
$BaCo_{0.7}(Ce_{0.8}Y_{0.2})_{0.3}O_{3-\delta}$	BZCY172	Air, 3% H_2O	650	0.145	This work
			600	0.325	
			550	0.868	
	BZCYYb1711	Dry Air	650	0.17	1
			600	0.51	
			550	1.53	
		Air, 5% H_2O	650	0.06	
			600	0.11	
			550	0.20	
$La_{0.8}Sr_{0.2}MnO_3$	BZCY172	Air, 3% H_2O	650	2.244	This work
			600	6.888	
			550	20.950	
	BZCY172	Ambient air	650	1.84	2
			600	5.33	
			550	16.88	
$BaCo_{0.4}Fe_{0.4}Zr_{0.1}Y_{0.1}O_{3-\delta}$	BZCY172	Air, 3% H_2O	650	0.251	This work
			600	0.480	
			550	1.283	
	BZCY172	Air, 10% H_2O	650	0.142	3
			600	0.274	
			550	0.693	
$PrBa_{0.5}Sr_{0.5}Co_{1.5}Fe_{0.5}O_{5+\delta}$	BZCY172	Air, 3% H_2O	650	0.353	This work
			600	1.080	
			550	3.729	
	BZCYYb1711	Air, 3% H_2O	650	0.35	4
			600	1.04	
			550	2.34	

Table S2. Comparison of the different electrode ASRs measured based on SDC/GDC electrolyte symmetric cells in the temperature range of 550 to 650 °C in this work with the estimated values reported in the literature.

Cathode	Electrolyte	Atmosphere & humidity	Temperature (°C)	ASR (Ω cm^2)	Ref.
$BaCo_{0.7}(Ce_{0.8}Y_{0.2})_{0.3}O_{3-\delta}$	SDC	Air, 3% H_2O	650	0.223	This work
			600	0.664	
			550	1.936	
	SDC	Ambient air	650	0.018	[1]
			600	0.034	
			550	0.076	
$La_{0.8}Sr_{0.2}MnO_3$	SDC	Air, 3% H_2O	650	38.341	This work
			600	97.561	
			550	270.998	
	GDC	Ambient air	650	4.103	[5]
			600	8.312	
			550	15.94	
$BaCo_{0.4}Fe_{0.4}Zr_{0.1}Y_{0.1}O_{3-\delta}$	SDC	Air, 3% H_2O	650	0.022	This work
			600	0.052	
			550	0.164	
	GDC	Ambient air	600	0.29	[6]
			550	0.6	
			500	1.24	
$PrBa_{0.5}Sr_{0.5}Co_{1.5}Fe_{0.5}O_{5+\delta}$	SDC	Air, 3% H_2O	650	0.034	This work
			600	0.083	
			550	0.222	
	GDC	Ambient air	650	0.058	[7]
			600	0.104	
			550	0.235	

Table S3. ICP-OES results of the synthesized SDC and BZCY electrolytes.

Sample	Theoretical atomic ratio	Tested atomic ratio
SDC	0.2 : 0.80 (Sm : Ce)	0.197 : 0.803 (Sm : Ce)
BZCY	1.00 : 0.10 : 0.70 : 0.20 (Ba : Z r: Ce : Y)	1.00 : 0.098 : 0.708 : 0.194 (Ba : Zr : Ce : Y)

Table S4. Electrochemical characterization of the representative cells in this work compared with corresponding cells reported in the literatures.

Single cell configuration			Atmosphere		Electrolyte Conductivity (mS cm-1)				Ref
Anode	Electrolyte	Cathode	Anode	Cathode	650 (°C)	600 (°C)	550 (°C)	500 (°C)	
BCCY	BZCY172 [~900 μm]	BCCY	3% H_2O, 20 mL min^{-1} Air	3% H_2O, 20 mL min^{-1} Air	42.29	33.19	25.11	18.08	This work
BCCY	SDC [~850 μm]	BCCY	3% H_2O, 20 mL min^{-1} Air	3% H_2O, 20 mL min^{-1} Air	58.91	37.30	21.81	11.45	
NiO-BZCY172	BZCY172 [25 μm]	BCCY	3% H_2O, 100 mL min^{-1} H_2	Ambient Air	8.09	7.06	5.97	4.91	
NiO-BZCY442	BZCY442 [16 μm]	BCCY	80 mL min^{-1} H_2	Ambient Air	4.03	3.29	2.93	/	[1]
NiO-BZCY1711	BZCY1711 [16 μm]	BCCY	80 mL min^{-1} H_2	Ambient Air	10.39	8.05	6.44	/	
LSM	BZCY172 [~900 μm]	LSM	3% H_2O, 20 mL min^{-1} Air	3% H_2O, 20 mL min^{-1} Air	56.04	37.38	21.97	11.61	This work
LSM	SDC [~850 μm]	LSM	3% H_2O, 20 mL min^{-1} Air	3% H_2O, 20 mL min^{-1} Air	36.64	28.92	22.22	15.60	
NiO-BZCY172	BZCY172 [25 μm]	LSM	3% H_2O, 100 mL min^{-1} H_2	Ambient Air	7.62	6.46	5.37	4.15	
NiO-BZCY172	BZCY172 [12.5 μm]	LSM	3% H_2O, 30 mL min^{-1} H_2	Ambient Air	5.06	4.07	3.06	/	[2]
BCFZY	BZCY172 [~900 μm]	BCFZY	3% H_2O, 20 mL min^{-1} Air	3% H_2O, 20 mL min^{-1} Air	60.24	37.79	21.64	11.18	This work
BCFZY	SDC [~850 μm]	BCFZY	3% H_2O, 20 mL min^{-1} Air	3% H_2O, 20 mL min^{-1} Air	41,78	32.85	25.06	17.49	
NiO-BZCY172	BZCY172 [23 μm]	BCFZY	3% H_2O, 100 mL min^{-1} H_2	Ambient Air	7.92	6.84	5.85	4.74	
NiO-BZCYYb1711	BZCY1711 [25 μm]	BCFZY	Dry 20 mL min^{-1} H_2	Dry Air, 100 mL min^{-1}	/	6.25	5.81	4.69	[8]
Ni−BZCYYbPd	BZCYYbPd [17 μm]	BCFZY	Dry 80 mL min^{-1} H_2	Ambient Air	5.31	4.72	3.86	/	[9]
PBSCF	BZCY172 [~900 μm]	PBSCF	3% H_2O, 20 mL min^{-1} Air	3% H_2O, 20 mL min^{-1} Air	60.33	38.01	22.16	11.72	This work

PBSCF	SDC [~850 µm]	PBSCF	3% H_2O, 20 mL min^{-1} Air	3% H_2O, 20 mL min^{-1} Air	39.68	30.80	23.25	16.88	
NiO-BZCY172	BZCY172 [22 µm]	PBSCF	3% H_2O, 100 mL min^{-1} H_2	Ambient Air	7.85	6.69	5.59	4.43	
NiO-BZCY1711	BZCY1711 [7 µm]	PBSCF	3% H_2O, 30 mL min^{-1} H_2	Ambient Air	5.71	5.33	4.21	/	4
NiO-BZCYYb2611	BZCYYb2611 [7.6 µm]	PBSCF	3% H_2O, 150 mL min^{-1} H_2	Dry Air, 200 mL min^{-1}	/	4.29	3.80	2.19	10

Estimated value from EIS plots in reported single cell electrochemical characterization.BZCY172: $BaZr_{0.1}Ce_{0.7}Y_{0.2}O_{3-\delta}$; BZCYYb1711: $BaZr_{0.1}Ce_{0.7}Y_{0.1}Yb_{0.1}O_{3-\delta}$; BZCYYv4411: $BaZr_{0.4}Ce_{0.4}Y_{0.1}Yb_{0.1}O_{3-\delta}$; BZCY442: $BaZr_{0.4}Ce_{0.4}Y_{0.2}O_{3-\delta}$; BZCYYb2611: $BaZr_{0.2}Ce_{0.6}Y_{0.1}Yb_{0.1}O_{3-\delta}$.

Reference

1. Y. Song, Y. Chen, W. Wang, C. Zhou, Y. Zhong, G. Yang, W. Zhou, M. Liu and Z. Shao, *Joule*, 2019, **3**, 2842-2853.
2. J. Hou, Q. Wang, J. Li, Y. Lu, L. Wang, X.-Z. Fu and J.-L. Luo, *J. Power Sources*, 2020, **466**, 228240.
3. R. Ren, Z. Wang, C. Xu, W. Sun, J. Qiao, D. W. Rooney and K. Sun, *J. Mater. Chem. A*, 2019, **7**, 18365-18372.
4. H. Zhang, K. Xu, F. He, Y. Zhou, K. Sasaki, B. Zhao, Y. Choi, M. Liu and Y. Chen, *Adv. Energy Mater.,* 2022, **12**, 2200761.
5. N. Li, L. Sun, Q. Li, T. Xia, L. Huo and H. Zhao, *J. Eur. Ceram. Soc.,* 2023, **43**, 5279-5287.
6. C. Duan, D. Hook, Y. Chen, J. Tong and R. O'Hayre, *Energy Environ. Mater.*, 2017, **10**, 176-182.
7. S. Park, S. Choi, J. Shin and G. Kim, *RSC Adv.*, 2014, **4**, 1775-1781.
8. C. Duan, J. Tong, M. Shang, S. Nikodemski, M. Sanders, S. Ricote, A. Almansoori and R. O' Hayre, *Science,* 2015, **349**, 1321-1326.
9. F. He, Q. Gao, Z. Liu, M. Yang, R. Ran, G. Yang, W. Wang, W. Zhou and Z. Shao, *Adv. Energy Mater.*, 2021, **11**, 2003916.
10. E. H. Kang, H. R. Choi, J. S. Park, K. H. Kim, D. H. Kim, K. Bae, F. B. Prinz and J. H. Shim, *J. Power Sources*, 2020, **465**, 228254.